

RESEARCH

Open Access



# Toxic effects of prolonged propofol exposure on cardiac development in zebrafish larvae

Shaojie Qian<sup>1</sup>, Huizi Liu<sup>1</sup>, Hanwei Wei<sup>1</sup>, Jintao Liu<sup>1</sup>, Xiaojun Li<sup>1</sup> and Xiaopan Luo<sup>1\*</sup>

## Abstract

**Background** Propofol, commonly used as an intravenous anesthetic during pregnancy, can easily penetrate the placental barrier, potentially affecting fetal heart development. This study aims to investigate propofol's impact on developing zebrafish heart structure and function, and identify potential drug targets.

**Methods** Zebrafish embryos were exposed to different concentrations of propofol (0.5, 1, and 5 mg/L) to observe changes in zebrafish larval heart structure and function (heart rate). In vitro cell experiments were conducted to assess the effects of propofol at different concentrations on cardiomyocyte viability and migration. Transcriptomic sequencing was utilized to identify and validate potential drug targets associated with propofol-induced cardiac toxicity.

**Results** The results demonstrate that propofol dose-dependently reduces the hatching and survival rates of zebrafish larvae, while increasing the rate of deformities. Transgenic green fluorescent zebrafish larvae exposed to propofol exhibit enlarged cardiac cavities, and HE staining reveals thinning of the myocardial wall. Additionally, propofol-treated zebrafish larvae show a decrease in heart rate. We also assess the impact of propofol on myocardial cell function, showing decreased cell viability, reduced migration function, and increased apoptosis. Finally, transcriptome sequencing analysis and differential gene co-expression network analysis identify *agxt2* as a potential target of propofol-induced cardiac toxicity.

**Conclusion** In conclusion, our study indicates that propofol alters the structure and function of the developing zebrafish heart, with the mitochondrial-related gene *agxt2* possibly being a target of its pharmacological effects.

**Keywords** Propofol, Cardiotoxicity, Heart development, Embryo development

## Introduction

Approximately 0.75-2% of pregnant women receive non-obstetric surgery under general anesthesia each year [1]. Although general anesthetics have been safely used for surgeries for decades, their effects on developing organs such as the brain and heart are raising concerns when

used during pregnancy. Propofol, the most common intravenous general anesthetic in clinical use, can easily move from the placenta into the fetal blood circulation due to its high solubility in lipids [2]. Due to its fast action and breakdown, propofol is a common choice for general anesthesia in laparoscopic surgery during pregnancy. The guidelines also recommend propofol for endoscopy anesthesia during pregnancy [3]. Thus, propofol's impact on fetal organ development requires attention.

Both clinical and animal evidence indicate that early life exposure to propofol could adversely affect fetal cardiac development. For example, Prolonged propofol

\*Correspondence:

Xiaopan Luo  
luoxiaop12@163.com

<sup>1</sup>Center for Rehabilitation Medicine, Department of Anesthesiology, Zhejiang Provincial People's Hospital, Affiliated People's Hospital, Hangzhou Medical College, Hangzhou, Zhejiang, China



© The Author(s) 2025. **Open Access** This article is licensed under a Creative Commons Attribution-NonCommercial-NoDerivatives 4.0 International License, which permits any non-commercial use, sharing, distribution and reproduction in any medium or format, as long as you give appropriate credit to the original author(s) and the source, provide a link to the Creative Commons licence, and indicate if you modified the licensed material. You do not have permission under this licence to share adapted material derived from this article or parts of it. The images or other third party material in this article are included in the article's Creative Commons licence, unless indicated otherwise in a credit line to the material. If material is not included in the article's Creative Commons licence and your intended use is not permitted by statutory regulation or exceeds the permitted use, you will need to obtain permission directly from the copyright holder. To view a copy of this licence, visit <http://creativecommons.org/licenses/by-nc-nd/4.0/>.

infusion can cause propofol infusion syndrome, which leads to cardiac dysfunction and arrhythmia [4]. Specifically, propofol infusion syndrome is more likely to occur in younger patients [5]. This is the clinical manifestation of propofol mediated cardiotoxicity. Additionally, in a newborn mouse heart model of propofol-induced cardiotoxicity, a high dose of propofol quickly triggered arrhythmias, reduced ventricular contractility, compromised mitochondrial function, and enhanced permeability transition pore opening [6]. Besides, our previous study showed that zebrafish larvae exposed to 5 mg/L of propofol reduce SV-BA distance and slower heart rates [7].

Numerous studies have explored the mechanisms of propofol-induced cardiotoxicity. The mechanisms can be divided into two main categories. The first one involves mitochondria. By affecting oxygen use or blocking electron movement in the mitochondrial electron transport chain, propofol weakens the guinea pig heart cell [8]. It also lowers the ventricular function of the isolated perfused heart. In a cardiomyocyte model of propofol-induced cytotoxicity established by human-induced pluripotent stem cells, propofol above 10 mg/L caused mitochondrial dysfunction and lowered the activity of PGC-1 $\alpha$  and its related genes [9]. Another study showed that propofol disrupted immature cardiomyocyte mitochondria by causing too much coenzyme Q sensitive leak and blocking electron flow at coenzyme Q [10]. This revealed how propofol harmed the developing heart and why children were prone to PRIS. The second one involves heart ion channels. Propofol blocks many types of ion channels, such as calcium and potassium channels [11, 12]. This could lead to propofol-induced clinical bradycardia. Although propofol-induced cardiotoxicity has been investigated by many studies, the mechanism and target of cardiotoxicity of propofol in the developing heart remain unclear.

Zebrafish, a common model organism, is used to study development, genetics, and toxicity [13]. It is also suitable for exploring the heart's function and development. In this study, we exposed juvenile zebrafish to propofol and observed changes in their heart structure and function. We then performed transcriptome gene sequencing on their heart tissue and analyzed the data using differential gene PPI network analysis. This helped us identify potential targets of propofol-induced cardiotoxicity during development.

## Materials and methods

### Zebrafish cultivation and egg production

Transgenic Tg[*myl7:eGFP*] and wild-type AB strain zebrafish from China Zebrafish Resource Center were housed in a recirculating water system at 28 °C with a 14:10-h light/dark cycle and fed thrice daily. Overnight

pairing of male and female zebrafish produced embryos, which were collected within 1 h of light onset and incubated in 10-cm Petri dishes with egg water and methylene blue (0.3 ppm) at 28 °C under a 14:10-h light/dark cycle. Based on a previous study, embryos were treated with 0.5, 1, and 5 mg/L propofol dissolved in 0.01% dimethyl sulfoxide (DMSO) at 8 h post-fertilization (hpf) [7]. Glass petri dishes were used as carriers. An incubation solution with 0.01% DMSO served as the control group (CK). Ten embryos per group were placed in six-well plates with 6 ml of test solution and each group was replicated thrice. Hatchability, death rate, and malformation rate of zebrafish at 24, 48, 72, 96, and 120 hpf were recorded. Half of the solution was replaced every two days to maintain propofol concentration and feeding was stopped 24 h before the experiment. The Institutional Animal Care and Use Committee of Affiliated People's Hospital, Hangzhou Medical College, Hangzhou, China approved all procedures.

### Histology

Embryos from both the control and treatment groups at 72 hpf were selected based on their normal or severe deformity. They were fixed in 4% paraformaldehyde at 4 °C overnight and washed with PBS three times for 5 min each. Paraffin sections and staining followed the previously reported procedure [14].

### Zebrafish hearts isolation

Zebrafish embryonic heart dissection was performed according to a previously published protocol [15]. Briefly, 100 Tg[*myl7:eGFP*] zebrafish embryos at 96 hpf from control group or propofol group were collected respectively, and transferred into 1.5 mL tube on ice. To disrupt the embryos and the yolk, added 1 mL L-15/10% FBS medium and pipetted them 5–8 times with a Round Gel Loading Tip, then dropped them onto the solution surface. The embryos pericardial cavity was destroyed using a 1 mL syringe with a 25G needle. GFP-positive hearts were manually separated under a fluorescence stereomicroscope and collected into L-15/10% FBS medium for further study.

### CCK-8 assay

After digestion and centrifugation, H9C2 cells were resuspended to a density of  $3 \times 10^4$  cells/ml. A 100  $\mu$ l cell suspension was added to each well of a 96-well plate. Following overnight pre-incubation at 37 °C, various concentrations of propofol were added and incubated for 72 h at 37 °C. Subsequently, 10  $\mu$ l of CCK-8 solution (vazyme, A311-02) was added to each well and incubated for 2 h, followed by measurement of OD values at 450 nm to assess cell viability.

### Cell transwell assay

Matrigel stored at  $-20^{\circ}\text{C}$  was thawed overnight at  $2^{\circ}\text{C}\sim 8^{\circ}\text{C}$  on ice, diluted 1:3 in pre-chilled serum-free medium, and mixed thoroughly. The diluted Matrigel was applied to the upper chamber of Transwell plates to coat the polycarbonate membrane and allowed to polymerize at  $37^{\circ}\text{C}$  for 30 min. Drug-treated cells were digested, centrifuged, resuspended in serum-free medium, and adjusted to the desired density. Transwell chambers were then placed in a 24-well plate with complete medium in the lower chamber. After 24 h, the upper chamber was removed, medium discarded, and chambers rinsed twice with PBS. Matrigel and surface cells were gently wiped, fixed in 4% paraformaldehyde for 20 min, washed twice with PBS, stained with crystal violet for 10 min, and rinsed with water. Cells that migrated through the Transwell membrane were counted under a microscope.

### Tunel assay

Briefly, the cell samples were fixed with 4% paraformaldehyde at room temperature for 20–30 min and then treated with 1% Triton X-100 permeabilization solution at room temperature for 3–5 min. Next, DNase I reaction solution was added to each sample and incubated at  $37^{\circ}\text{C}$  for 30 min. TdT enzyme reaction solution was added to each sample, followed by incubation in a dark chamber at  $37^{\circ}\text{C}$  for 30–60 min. Streptavidin-FITC labeling solution was added to each sample, followed by incubation in a humid chamber at  $37^{\circ}\text{C}$  for 30 min in the dark. Nuclei were counterstained with DAPI staining solution, incubated at room temperature in the dark for 10 min. Excess DAPI staining solution was washed off, and mounting medium was applied for microscopy observation.

### RNA-seq and bioinformatic analysis

At 96 hpf, each group (5 mg/L propofol and control) consisted of 60 zebrafish larvae, from which hearts were dissected and extracted for RNA sequencing. Three biological replicates were included per group ( $n=3$ ). After zebrafish embryonic hearts were isolated, total RNA was extracted from two group samples of zebrafish embryonic hearts using TRIzol (Thermo Fisher Scientific, USA), including control group and propofol group, respectively. Qualified total RNA was selected as the starting sample for mRNA sequencing library preparation. The quality requirements were a RIN (RNA Integrity Number)  $\geq 7$ , with the ratio of 28 S to 18 S RNA  $\geq 1.5:1$ , as determined by the Agilent 2100 BioAnalyzer (USA). The total RNA was accurately quantified using the Qubit RNA Assay Kit (Thermo Fisher Scientific, USA). The cDNA libraries were constructed by using NEBNext Ultra™ RNA Library Prep Kit for Illumina (NEB, USA) and sequenced by Illumina BioelectronSeq 4000 platform (CapitalBio

Technology, China). The sequencing reads were mapped to Danio rerio reference genome (NCBI\_GRCz11).

Differential expressed genes (DEGs) analysis of the two groups was analyzed using the TBtools software (version 2.019) [16]. The  $p$  values were adjusted using the Benjamini and Hochberg's approach for controlling the false discovery rate. Genes with an adjusted  $p$  value  $< 0.05$  and  $|\log_2(\text{Fold change})| \geq 2$  were considered as differentially expressed.

The DEGs were subjected to enrichment analyses of Gene Ontology (GO) and KEGG pathways analysis. GO terms and KEGG analysis with corrected  $p$  value  $< 0.05$  were considered as significantly enriched. Volcano plots were generated by Origin (version 10.1). PPI networks were drawn using Cytoscape (version 3.4.2) and hub genes were identified.

### Western blot

Zebrafish embryonic hearts from control or propofol groups were dissected at 96hpf and protein was extracted from 100 pooled hearts. Each protein lysate was boiled in 3x Loading Buffer and loaded on a 10% SDS gel (Bio-Rad). Proteins were separated by SDS-PAGE and transferred to a PVDF membrane. The membrane was blocked in 5% milk/TBST for 2 h at RT, incubated with the primary antibody at  $4^{\circ}\text{C}$  overnight, and then with the secondary antibody for 2 h at RT. Antibodies used for these experiments were anti-agxt2 (1:1000; ab237622, Abcam), anti-GAPDH (1:1000; #5174S, Cell Signaling Technology). Signal detection was carried out using the enhanced chemiluminescent substrate SuperSignal™ West Femto (Thermo Fisher Scientific, USA). Signal intensities, quantified by the software ImageJ, were normalized to their loading control (GAPDH).

### Statistical analysis

Data are presented as mean  $\pm$  SD. Statistical differences between two or more groups were determined using the Student's  $t$ -test and one-way ANOVA followed by the Student-Newman-Keuls test, respectively. All experiments were repeated at least three times. A  $P$ -value  $< 0.05$  was considered to indicate statistical significance.

## Results

### Developmental toxicity of propofol in zebrafish embryos

To investigate the developmental toxicity of propofol on zebrafish embryos, the survival rate, hatching rate and malformation rate were recorded at 24, 48, 72, 96 and 120 hpf. Our results indicated that there was no significant decrease of the survival rates and hatching rates following exposure to propofol in the control and 0.5 mg/L groups (Fig. 1A and B). In the 1 mg/L treatment group, there was a significant increase in death rates from 72 hpf, whereas in the 5 mg/ml treatment group, there was a significant

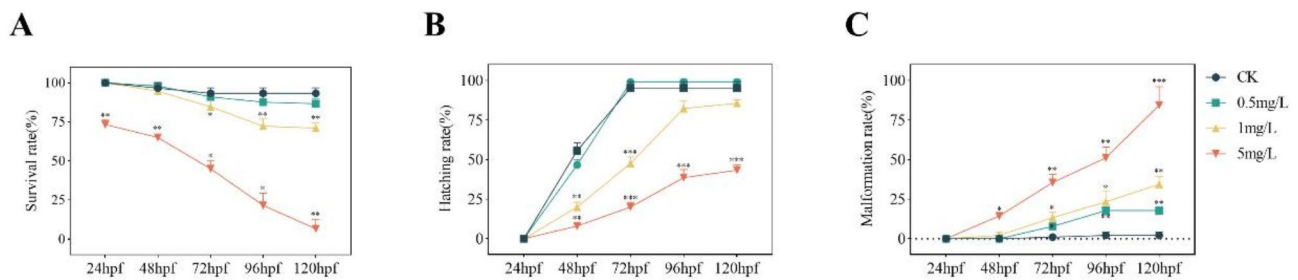


**Fig. 1** Propofol causes noticeable developmental toxicity in zebrafish larvae. Survival rates (A), hatching rates (B) and malformation rates (C) of zebrafish embryos exposed to propofol at 24, 48, 72, 96 and 120 hpf. Data shown as the means  $\pm$  standard deviation (SD), ( $n = 3$ ). \* $p < 0.05$ , \*\* $p < 0.01$ , \*\*\* $p < 0.001$  vs. control

decrease in survival rates from 24 hpf (Fig. 1A). The hatching rate was significantly decreased in the 1 mg/L and 5 mg/L propofol-treated groups compared with the control from 48 hpf (Fig. 1B). However, severe malformation of all embryos at 72 hpf was observed in 0.5, 1, and 5 mg/L propofol groups (Fig. 1C) and the malformation rates presented in a dose-dependent manner. These developmental toxic effects induced by propofol are consistent with our previous findings [7].

#### Propofol exposure causes significant changes in zebrafish heart structure and function

Treatment of zebrafish embryos with different concentrations of propofol resulted in obvious cardiac malformation phenotypes, especially a relatively high proportion of pericardial cysts (Fig. 2A). The proportion of cardiac malformations increases with the exposure concentration, showing a significant dose-dependent phenotype (Fig. 2B). In order to study the damage of propofol to zebrafish heart development, propofol was exposed to Tg[myl7:eGFP] transgenic zebrafish to observe the morphological changes of the heart. It was found that propofol exposure caused obvious cardiac development abnormalities, including prolonged pericardium and increased pericardial cysts, and the atrial and ventricular spaces were significantly enlarged. In the normal group, the overlap of the atria and ventricles and the circularization of the heart can be clearly observed. However, in the propofol treatment group, the overlapping capacity of the atria and the ventricle was reduced, and the degree of cyclization was reduced, especially in the high concentration treatment group (Fig. 2C and D).

In order to observe the changes in the structure of the heart after propofol exposure, HE staining of tissue sections was used to observe the changes in the structure of the heart. As a result, it was found that the tissues of the heart were severely damaged after propofol exposure, and as the exposure concentration increased, the damage became more serious. As the exposure concentration increases, the myocardial wall of the heart muscle thickens significantly, and the atrium and ventricular

cavity decreases (Fig. 2E). These data indicate that propofol causes obvious damage to the developmental morphology of the zebrafish heart. Propofol administration at both 1 mg/L and 5 mg/L significantly decreased the heart rate compared to the control and 0.5 mg/L groups (Fig. 2F).

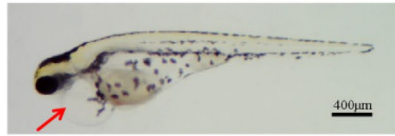
#### Propofol inhibits cardiomyocyte viability, migration and promotes apoptosis

To investigate the impact of propofol on cardiomyocytes, we conducted experiments assessing cell viability, migration, and apoptosis. As propofol concentration increased, cardiomyocyte activity decreased in a concentration-dependent manner. Specifically, at a propofol concentration of 5 mg/L (Fig. 3A), cell viability decreased by 24.93% compared to the control group. Additionally, using the Trans-well assay, we observed that higher propofol concentrations correlated with fewer migrated cells (Fig. 3B and C). Furthermore, our TUNEL experiment demonstrated an increase in apoptosis with rising propofol concentration. Compared to the control group, apoptosis rose by 15.83% at 5 mg/L (Fig. 3D and E). In summary, elevated propofol concentration hindered cardiomyocyte viability and migration while promoting apoptosis.

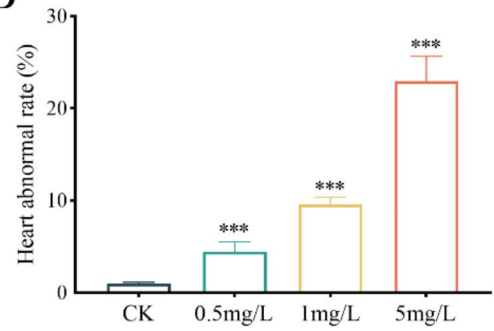
#### Transcriptome sequencing to analyze the mechanism of propofol-induced heart damage in zebrafish

To investigate the molecular mechanism underlying myocardial damage caused by propofol in developing zebrafish larvae, we employed Illumina transcriptome sequencing to analyze the transcriptomes of zebrafish cardiomyocytes from both the control group and the propofol-treated group (5 mg/L). Our differential gene analysis revealed 1102 up-regulated genes and 1328 down-regulated genes (Fig. 4A). Subsequently, we performed GO and KEGG pathway enrichment analyses, highlighting cell biological process, cellular component, molecular function, and signaling pathways (as depicted in Fig. 4B). To identify potential targets of propofol-induced cardiomyocyte toxicity, we conducted weighted gene co-expression network analysis

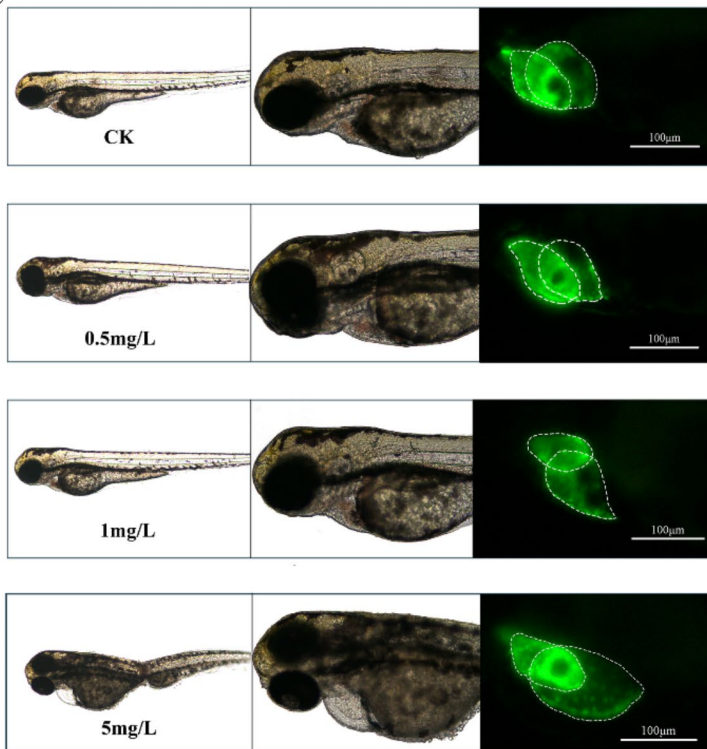
A



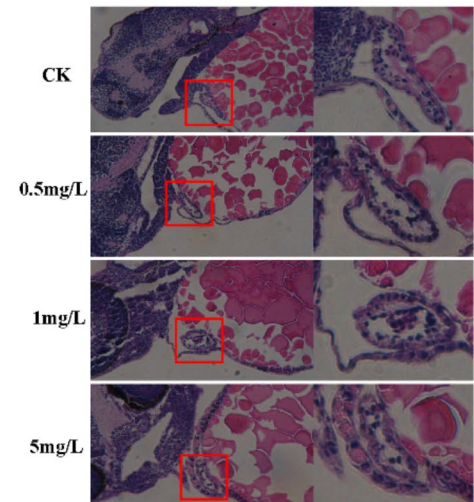
B



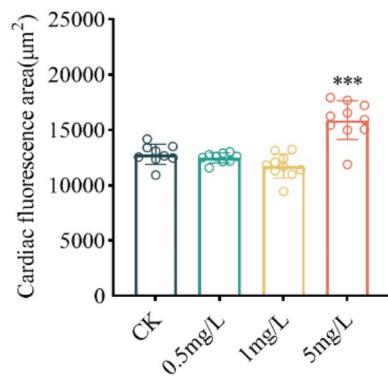
C



E



D



F

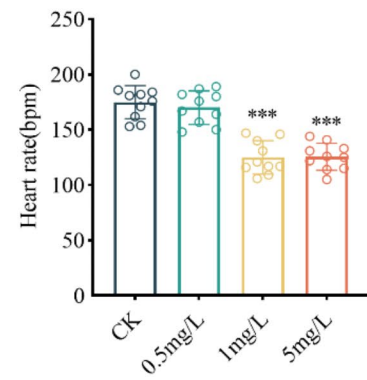


Fig. 2 (See legend on next page.)

(See figure on previous page.)

**Fig. 2** Propofol alters heart structure and function (heart rate) in zebrafish larvae. **(A)**. Propofol-induced pericardial cyst in zebrafish larvae at 96hpf. **(B)**. The incidence of propofol-induced heart malformations rose with higher concentrations. Cardiac malformations are defined as the observation of pericardial edema, abnormal chamber size, pericardial extension, and irregular heart morphology. **(C)**. Cardiac morphology changes in Tg [*myl7:eGFP*] zebrafish larvae exposed to varying propofol concentrations included reduced atrioventricular overlap, prolonged pericardium, and enlarged cardiac cavity area. **(D)**. Cardiac fluorescence area. **(E)**. Representative images of HE-stained zebrafish embryo hearts following propofol exposure. **(F)**. Heart rate changes in zebrafish larvae treated with different concentrations of propofol. Data are presented as the means  $\pm$  SD of at least three independent experiments. Student's t-test statistical analysis. \*\*\* $p < 0.001$  vs. control

using the differentially expressed genes. Remarkably, AGXT2 emerged as the central hub gene with the highest weight (Fig. 4C). Finally, Western blotting confirmed that AGXT2 protein expression was significantly reduced in the propofol group (Fig. 4D and E), consistent with the down-regulation observed in the transcriptome sequencing results. Thus, AGXT2 protein may serve as a promising target in propofol-induced myocardial developmental toxicity.

## Discussion

Propofol, due to its high lipid solubility, can easily traverse the placental barrier and enter the fetal bloodstream. The human heart is one of the earliest organs to form and function during embryonic development [17]. Currently, there is a lack of clinical evidence linking propofol exposure to congenital heart disease in humans. This study found that zebrafish larvae exposed to propofol exhibited decreased hatching rates, reduced survival rates, and increased deformity rates, indicating the developmental toxicity of propofol on zebrafish larvae, consistent with previous research findings. To further explore the effects of propofol exposure on cardiac structure and function during development, we conducted experiments using fluorescent zebrafish and HE staining, revealing alterations in zebrafish larval cardiac structure, including cardiac enlargement and thinning of the myocardial layer. Additionally, propofol inhibited the heart rate of zebrafish larvae and exerted toxic effects on cardiomyocytes, suppressing their vitality and migration while promoting apoptosis. Finally, through transcriptome gene sequencing and differential gene analysis, we identified the *agxt2* gene as a potential target of propofol-induced developmental toxicity in zebrafish hearts.

From the division and proliferation of the fertilized egg to the mature embryo, the heart is the earliest organ to form and function in the developmental process of vertebrate embryos [18]. During the early stages of embryonic development, the proliferation, migration, and differentiation of myocardial cells directly influence the morphology, size, and function of the mature heart. Previous studies have shown that propofol inhibits the proliferation, invasion, and differentiation of tumor cells and embryonic neural stem cells [19, 20]. Our study similarly found that propofol-treated myocardial cells exhibited a decreased proliferation rate, reduced migration function, and an increase in apoptosis rate with increasing

propofol concentration. This finding may explain the developmental cardiac structural abnormalities induced by propofol, such as increased cardiac chamber volume, thinning of the myocardial wall, and formation of pericardial cysts in zebrafish. Additionally, we observed that propofol can lower the heart rate of zebrafish. Previous research has indicated that propofol is toxic to developing neural cells and can inhibit neuronal electrical activity [21], which may account for the decreased heart rate in zebrafish, aligning with the clinical phenomenon of bradycardia following propofol anesthesia induction. Cardiac developmental abnormalities are widely regarded as fundamental causes of many congenital heart defects. Although our research suggests that propofol may lead to abnormalities in the structure and function of zebrafish embryo hearts during development, whether propofol is one of the causes of congenital heart diseases in clinical settings remains unclear. Currently, there is still a lack of definitive evidence in clinical settings linking propofol exposure during pregnancy to congenital heart diseases.

Although exposure to propofol during development may lead to cardiac toxicity, the specific mechanisms remain incompletely understood. Increasing evidence suggests that developmental cardiac toxicity induced by propofol is associated with mitochondrial dysfunction. For instance, in an ex vivo heart model of neonatal mice, the cardiac toxicity induced by high concentrations of propofol exposure may occur through the opening of mitochondrial proton leak channels (such as mPTP) and interference with mitochondrial electron transport [6]. Additionally, in a human-induced pluripotent stem cell model of cardiomyocytes, propofol-induced cardiac toxicity may be due to the downregulation of genes related to mitochondrial energy metabolism [9]. Our study identified differential genes through transcriptome sequencing analysis and found that the *agxt2* gene related to mitochondria plays a crucial role through weighted gene co-expression network analysis. The *agxt2* gene is expressed in the liver, kidney, and heart, and its encoded protein is exclusively located in mitochondria [22]. This protein encoded by the gene can utilize methylarginine, such as asymmetric dimethylarginine (ADMA), as an amino donor and is therefore called dimethylarginine-pyruvate transaminase [23]. In mice with *agxt2* gene knockout, the expression levels of ADMA in plasma significantly increased [24]. The increase in ADMA directly promotes the generation of reactive oxygen species (ROS) [25],

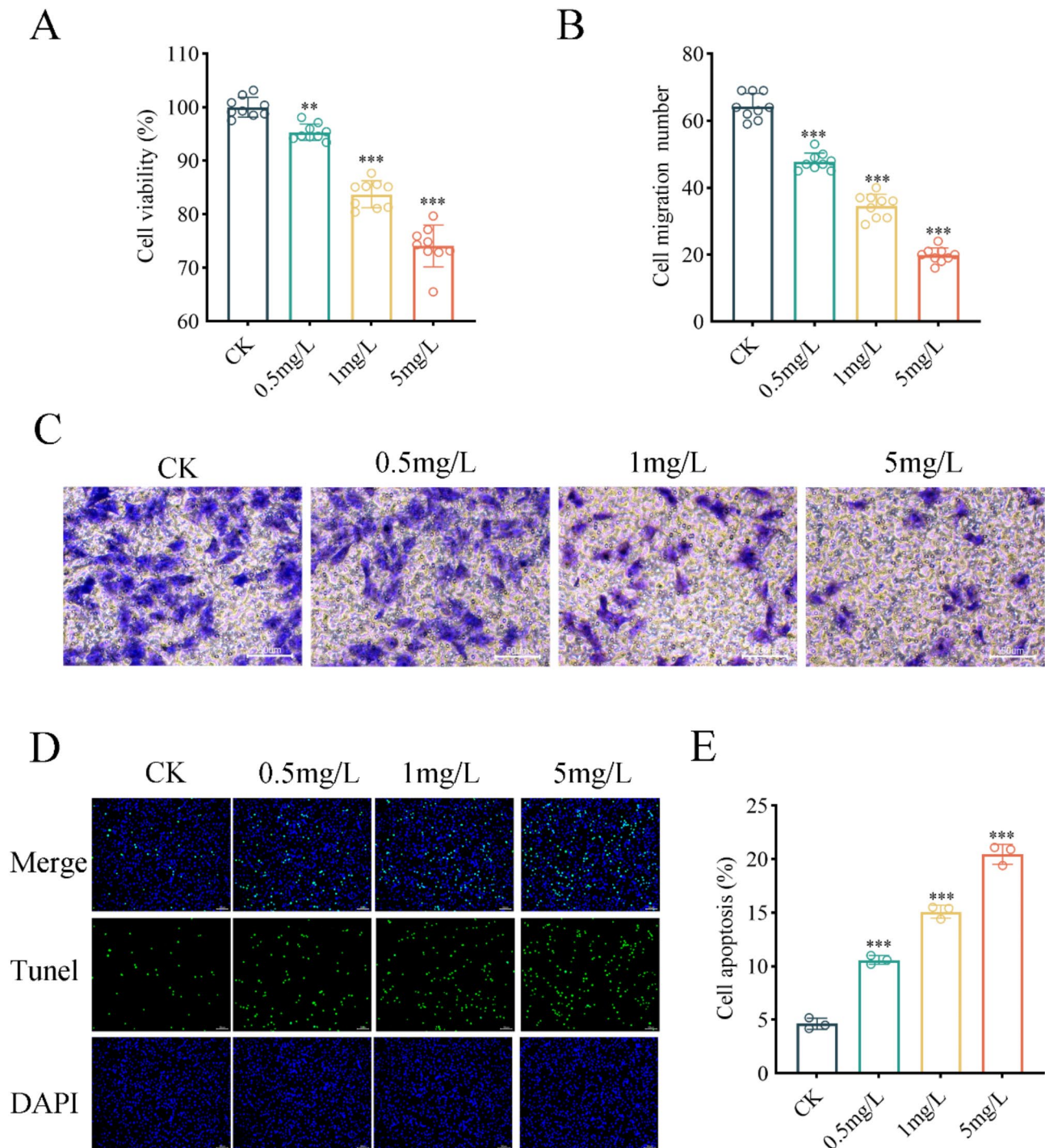


**Fig. 3** Propofol inhibits H9C2 cardiomyocyte viability, migration, and induces apoptosis. Propofol inhibited cell viability (**A**) and migration (**B**) in a concentration-dependent manner. Representative images from Transwell assays (**C**) illustrate its impact on cell migration, and TUNEL assays (**D**) demonstrate propofol-induced apoptosis, which increased with higher concentrations (**E**). Data shown as the means  $\pm$  SD, ( $n=3$ ). Scale bars = 50  $\mu$ m. \*\* $p < 0.01$ , \*\*\* $p < 0.001$  vs. control

thereby causing mitochondrial dysfunction and activating mitochondria-dependent cell apoptosis. In our study, we validated at the protein level that propofol can down-regulate the expression of agxt2. Therefore, we speculate that propofol may induce cardiac toxicity through the

agxt2/ADMA/ROS axis, but this needs further experimental verification. However, previous studies have shown that the drug toxicity of propofol may promote the production of ROS. In breast tumor cells, the dose-dependent effect of propofol increases ROS production

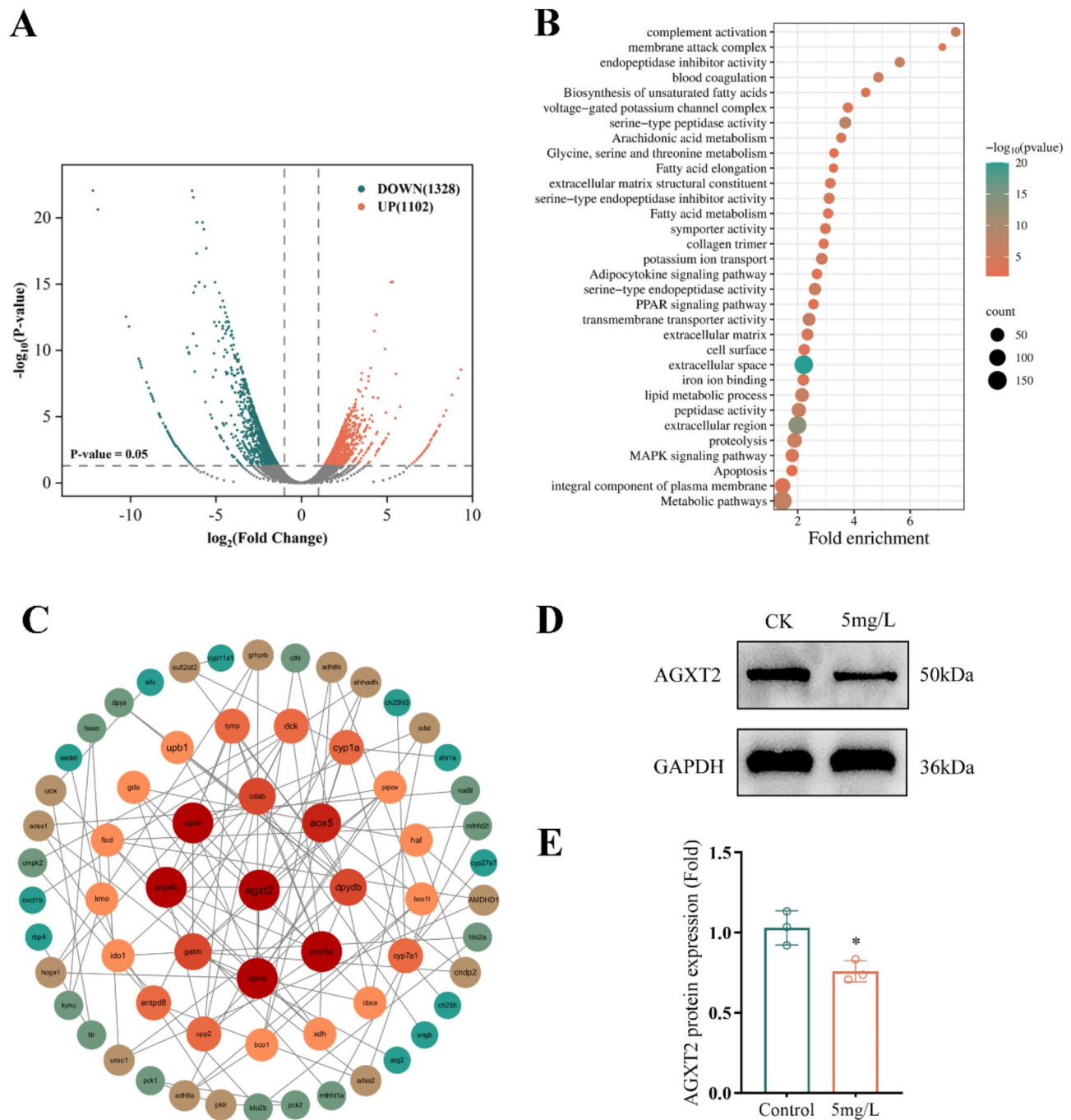


**Fig. 4** Transcriptome sequencing and differential gene analysis between 5 mg/L propofol-treated and control groups in zebrafish embryos. **(A)** The volcano plot highlights genes significantly altered in propofol-treated groups compared to controls ( $P\text{-values} < 0.05$ , fold change  $> 2$ ). Cyan and orange indicate down-regulated and up-regulated genes, respectively. **(B)** GO and KEGG enrichment analysis comparing control and propofol treatment groups. **(C)** The PPI network of DEGs. The PPI network was displayed by Cytoscape software. The hub genes were chosen based on a higher number of associations with other genes. **(D)** and **(E)** The protein expression of the hub gene AGXT2 was confirmed by western blot

[26]. Furthermore, exposure to propofol in zebrafish larvae during development causes oxidative damage to their embryos to a certain extent, and this oxidative damage exacerbates with increasing concentrations of propofol, showing a dose-response relationship [27].

Although we have observed that exposure to propofol can induce cardiotoxic effects in zebrafish larvae, there are some limitations in our study. Firstly, the duration of propofol exposure in our animal model was rather prolonged. In clinical practice, with the exception of its long-term use in sedation within ICU (intensive care unit), the

exposure of pregnant women to propofol typically does not exceed a few hours. To allow for the observation of more pronounced cardiotoxic effects, we opted for a longer exposure period in our research. Furthermore, we have identified the AGXT2 gene as a potential target for propofol-induced cardiac toxicity in zebrafish larvae. However, we have yet to explore its specific mechanisms in depth. This will be a key focus of our future research. Finally, we did not assess the metabolites of propofol or their effects on zebrafish larvae.

Exposure to propofol during development may have toxic effects on the heart, which requires careful attention. Clinically, the use of anesthetic drugs crossing the placental barrier from the early stages of embryo division to the end of pregnancy should be thoroughly evaluated for their potential toxicity to fetal organs. Particularly, propofol, as a primary drug for general anesthesia during pregnancy, necessitates further exploration of its effects on cardiac structure and function during embryonic development stages. In this study, we investigated the impact of propofol on the cardiac structure and function of zebrafish larvae and identified potential drug targets through transcriptome analysis, providing direction for future research.

## Conclusion

In our study, we observed changes in both the structure and function of the zebrafish larvae hearts following exposure to propofol. Additionally, we found that propofol exposure resulted in decreased apoptosis, proliferation, and migration capability of myocardial cells. Through transcriptomic analysis of differential gene expression, we also identified *agxt2* as a potential target of propofol-induced cardiac toxicity.

## Supplementary Information

The online version contains supplementary material available at <https://doi.org/10.1186/s12871-025-02942-1>.

Supplementary Material 1

## Acknowledgements

Not applicable.

## Author contributions

The first author, Shaojie Qian, and the corresponding author, Xiaopan Luo, conceived and designed the study. Shaojie Qian drafted the manuscript, which was revised by Xiaopan Luo. Animal experiments were conducted jointly by Shaojie Qian, Huizi Liu, and Hanwei Wei. Cell experiments were jointly conducted by Shaojie Qian and Jintao Liu. Data collection, analysis, and all software-generated figures were performed by Shaojie Qian and Xiaojun Li. Funding for the study was provided by Xiaopan Luo.

## Funding

This project received funding from grants provided by the Health Bureau (2020KY418, 2020KY450) and the Education Department (Y201942533) of Zhejiang Province.

## Data availability

The RNA-seq data has been deposited in the NCBI Gene Expression Omnibus database, with accession number PRJNA1161607.

## Declarations

### Ethics approval and consent to participate

The Institutional Animal Care and Use Committee of Affiliated People's Hospital, Hangzhou Medical College, Hangzhou, China approved all procedures.

### Consent for publication

Not applicable.

### Competing interests

The authors declare no competing interests.

Received: 4 August 2024 / Accepted: 3 February 2025

Published online: 18 February 2025

## References

1. Arkenbosch JHC, van Ruler O, de Vries AC. Non-obstetric surgery in pregnancy (including bowel surgery and gallbladder surgery). *Best Pract Res Clin Gastroenterol* 2020, 44–5.
2. Griffiths SK, Campbell JP. Placental structure, function and drug transfer. *Bja Educ*. 2015;15(2):84–9.
3. Qureshi WA, Rajan E, Adler DG, Davila RE, Hirota WK, Jacobson BC, Leighton JA, Zuckerman MJ, Hambrick RD, Fanelli RD, et al. ASGE Guideline: guidelines for endoscopy in pregnant and lactating women. *Gastrointest Endosc*. 2005;61(3):357–62.
4. Robinson JDC, Melman Y, Walsh EP. Cardiac conduction disturbances and ventricular tachycardia after prolonged propofol infusion in an infant. *Pace-Pacing Clin Electrophysiol*. 2008;31(8):1070–3.
5. Wolf A, Weir P, Segar P, Stone J, Shield J. Impaired fatty acid oxidation in propofol infusion syndrome. *Lancet*. 2001;357(9256):606–7.
6. Barajas MB, Wang AL, Griffiths KK, Sun LL, Yang G, Levy RJ. Modeling propofol-induced cardiotoxicity in the isolated-perfused newborn mouse heart. *Physiological Rep* 2022, 10(15).
7. Luo XP, Chen L, Zhang YL, Liu JT, Xie H. Developmental and cardiac toxicities of propofol in zebrafish larvae. *Comp Biochem Physiol C-Toxicology Pharmacol* 2020, 237.
8. Schenkman KA, Yan SL. Propofol impairment of mitochondrial respiration in isolated perfused guinea pig hearts determined by reflectance spectroscopy. *Crit Care Med*. 2000;28(1):172–7.
9. Kido K, Ito H, Yamamoto Y, Makita K, Uchida T. Cytotoxicity of propofol in human induced pluripotent stem cell-derived cardiomyocytes. *J Anesth*. 2018;32(1):120–31.
10. Vanlander AV, Okun JG, de Jaeger A, Smet J, De Lattre E, De Paepe B, Dacremont G, Wuyts B, Vanheel B, De Paepe P, et al. Possible pathogenic mechanism of Propofol Infusion Syndrome involves Coenzyme Q. *Anesthesiology*. 2015;122(2):343–52.
11. Zhou WG, Fontenot HJ, Liu S, Kennedy RH. Modulation of cardiac calcium channels by propofol. *Anesthesiology*. 1997;86(3):670–5.
12. Yang L, Liu H, Sun HY, Li GR. Intravenous anesthetic Propofol inhibits multiple human Cardiac Potassium channels. *Anesthesiology*. 2015;122(3):571–84.
13. Nishimura Y, Inoue A, Sasagawa S, Koiwa J, Kawaguchi K, Kawase R, Maruyama T, Kim S, Tanaka T. Using zebrafish in systems toxicology for developmental toxicity testing. *Congenit Anom*. 2016;56(1):18–27.
14. Hu N, Sedmera D, Yost HJ, Clark EB. Structure and function of the developing zebrafish heart. *Anat Rec*. 2000;260(2):148–57.
15. Lombardo VA, Otten C, Abdellilah-Seyfried S. Large-scale zebrafish embryonic heart dissection for transcriptional analysis. *Jove-Journal Visualized Experiments* 2015(95).
16. Chen CJ, Chen H, Zhang Y, Thomas HR, Frank MH, He YH, Xia R. TBtools: an integrative Toolkit developed for interactive analyses of big Biological Data. *Mol Plant*. 2020;13(8):1194–202.
17. Zaffran S, Frasch M. Early signals in cardiac development. *Circul Res*. 2002;91(6):457–69.

18. Fishman MC, Chien KR. Fashioning the vertebrate heart: earliest embryonic decisions. *Development*. 1997;124(11):2099–117.
19. Du Q, Liu J, Zhang XZ, Zhang X, Zhu H, Wei M, Wang SL. Propofol inhibits proliferation, migration, and invasion but promotes apoptosis by regulation of Sox4 in endometrial cancer cells. *Braz J Med Biol Res* 2018, 51(4).
20. Wang JW, Cheng WW, Xu T, Yang ZY. Propofol induces apoptosis and inhibits the proliferation of rat embryonic neural stem cells via gamma-aminobutyric acid type A receptor. *Genet Mol Res*. 2015;14(4):14920–8.
21. Twaroski DM, Yan YS, Zaja I, Clark E, Bosnjak ZJ, Bai XW. Altered mitochondrial dynamics contributes to Propofol-induced cell death in human stem cell-derived neurons. *Anesthesiology*. 2015;123(5):1067–83.
22. Rodionov RN, Jarzebska N, Weiss N, Lentz SR. AGXT2: a promiscuous aminotransferase. *Trends Pharmacol Sci*. 2014;35(11):31–8.
23. Hu XL, Li MP, Song PY, Tang J, Chen XP. AGXT2: an unnegligible aminotransferase in cardiovascular and urinary systems. *J Mol Cell Cardiol*. 2017;113:33–8.
24. Caplin B, Wang Z, Slaviero A, Tomlinson J, Dowsett L, Delahaye M, Salama A, Wheeler DC, Leiper J. Int Consortium Blood pressure G: alanine-glyoxylate Aminotransferase-2 metabolizes endogenous methylarginines, regulates NO, and controls blood pressure. *Arterioscler Thromb Vascular Biology*. 2012;32(12):2892–.
25. Wells SM, Holian A. Asymmetric dimethylarginine induces oxidative and nitrosative stress in murine lung epithelial cells. *Am J Respir Cell Mol Biol*. 2007;36(5):520–8.
26. Wang H, Zhao LD, Wu J, Hong J, Wang SP. Propofol induces ROS-mediated intrinsic apoptosis and migration in triple-negative breast cancer cells. *Oncol Lett*. 2020;20(1):810–6.
27. Jiang N, Li XX, Wang Q, Baihetiyaer B, Fan XT, Li MS, Sun HM, Yin XQ, Wang J. Ecological risk assessment of environmentally relevant concentrations of propofol on zebrafish (*Danio rerio*) at early life stage: insight into physiological, biochemical, and molecular aspects. *Chemosphere* 2023, 316.

### Publisher's note

Springer Nature remains neutral with regard to jurisdictional claims in published maps and institutional affiliations.